ACTA NEUROBIOLOGIAE EXPERIMENTALIS

Research paper Acta Neurobiol Exp 2015, 75: 351–363

Alteration of spontaneous spectral powers and coherences of local field potential in prenatal valproic acid mouse model of autism

Dania Cheaha and Ekkasit Kumarnsit*

Department of Physiology, Faculty of Science, Prince of Songkla University, Songkhla, Thailand,
*Email: kumarnsit.e@gmail.com

Previously, autism spectrum disorder (ASD) has been identified mainly by social communication deficits and behavioral symptoms. However, a link between behaviors and learning process in the brain of animal model of autism remained largely unexplored. Particularly, spontaneous neural signaling in learning-related brain areas has not been studied. This study investigated local field potential (LFP) of the hippocampus (HP), the olfactory bulb (OB) and the medial prefrontal cortex (mPFC) in mice prenatally exposed to valproic acid (VPA) on gestational day 13. Adult male Swiss albino mouse offspring implanted with intracranial electrodes were used. VPA-exposed mice exhibited ASD-associated behaviors. Hippocampal LFP analysis revealed that VPA group significantly increased low gamma activity (25–45 Hz) during awake immobility. Regression analyses confirmed positive correlations between locomotor speed and hippocampal theta oscillations in control but not VPA group. VPA group exhibited increases in delta (1–4 Hz) and beta (25–35 Hz) activities in OB during awake immobility and active exploring, respectively. Moreover, significantly increased and decreased coherences between HP and OB of VPA animals were seen within gamma (active exploration) and theta (awake immobility) ranges, respectively. In addition, significant increase in coherence between HP and mPFC was seen within delta range during active exploration. In addition to three ASD symptoms, VPA animals also exhibited differential patterns of olfacto-hippocampal LFP, altered locomotor speed-related hippocampal theta activities and distinct interplays between HP and learning-related brain areas. The altered olfacto-hippocampal and medial prefrontal cortex-hippocampal networks may underlie impairments in autism mouse model.

Key words: valproic acid, autism spectrum disorder, hippocampus, olfactory bulb, medial prefrontal cortex, local field potential

INTRODUCTION

Autism spectrum disorder (ASD) is a neurodevelopmental disorder collectively characterized by deficits in social communication and restricted/repetitive patterns of behavior (American Psychiatric Association 2013). However, ASD symptoms are considered heterogeneous and the identification remains to be improved for higher accuracy. Mainly, it is due to great complexity of ASD behavioral symptoms, complicated genetics and lack of reliable biomarkers. Therefore, modeling of human ASD in animals has been developed for better understanding of mechanisms underlying ASD pathogenesis and possible therapies.

Complex interactions between multiple susceptibility genes and environmental factors have been implicated in ASD (Chaste and Leboyer 2012, Volk et al. 2014). Prenatal exposure to chemical substances including thalidomide (Strömland et al. 1994, Miyazaki et al. 2005, Narita et al. 2010) or valproic acid (VPA), an anti-epileptic drug (Phiel 2001, Ornoy 2009), has been linked with increased risk of ASD. During embryogenesis, neural circuit development can be particularly sensitive to chemical teratogens (Rice and Barone 2000). Exposure to VPA during pregnancy causes fetal-valproate syndrome with autism-like

Correspondence should be addressed to E. Kumarnsit
Email: kumarnsit.e@gmail.com

Received 13 July 2015, accepted 29 November 2015

symptoms in human (Williams et al. 2001, Meador et al. 2009).

In animal studies, prenatal VPA exposure has been linked with well-replicated phenotypes that mimic the core symptoms of human autistic characters including deficits in social interaction, impaired ultrasonic vocalization and enhanced repetitive behaviors (Schneider and Przewłocki 2004, Kim et al. 2011, 2013). Consistent findings have also demonstrated remarkable similarities between autism cases and autism animal models. Abnormal expression of synaptic adhesion molecule neuroligin 3 has been observed in ASD subjects (Jamain et al. 2003, Shen et al. 2015) and VPA mouse model (Kolozsi et al. 2009, Gandal et al. 2010). Additionally, alterations in auditory function were also found both in ASD cases and VPA mouse model of ASD (Gandal et al. 2010). These indicate that ASD might be linked with changes in the central nervous system at multiple levels. Hence, an animal model of ASD with prenatal exposure to VPA appeared to be a plausible model for investigation of ASD-related neurobiological processes.

Consistent reports have confirmed the consequences of prenatal VPA exposure in various brain areas. Particularly, VPA-exposed animals were found to have structural and functional alterations in hippocampal networks (Bristot Silvestrin et al. 2013, Vorhees et al. 1991). In addition, olfactory dysfunctions have also been reported in VPA-exposed animals (Favre et al. 2013, Moldrich et al. 2013). Moreover, changes in synaptic plasticity in the medial prefrontal cortex were induced by prenatal exposure to VPA (Hara et al. 2015). These data indicate that the neural circuit networks are altered in VPA-exposed animals and might be associated with the core symptoms of ASD. However, no investigation of neural network activity has been performed in the areas particularly responsible for learning and memory processing.

Mostly, VPA rodent models have been identified using behavioral and molecular profiles associated with ASD symptoms. Electrophysiological biomarkers shared by animal models and patients with neurological disorders would be recognized as strong links between experimental and clinical research. Translational potential of electrophysiological biomarkers in both animal and human studies may be useful for diagnostic and therapeutic purposes. Neural network activities have also been investigated in mouse models of ASD induced by *in utero* VPA. In this model, neural circuit hyperactivity was observed in various brain areas including the somatosensory cortex, the prefrontal cortex (Silva et al. 2009) and the lateral amygdala (Markram et al. 2007). ASD may have distinct neural network function due to enriched ASD gene expression in superficial cortical layers and glutamatergic projection neurons (Willsey et al. 2013). Moreover, VPA animals also exhibited delayed auditory evoked-response endophenotypes (Gandal et al. 2010).

Recently, a VPA mouse model was found to have differential patterns of hippocampal and olfactory bulb LFPs in response to a new environment exposure (Cheaha et al. 2015). However, patterns of basal LFP in these learning-related brain areas of VPA-exposed animals in a familiar condition have not been studied. This study aimed to investigate the LFPs in order to search for biomarkers of the *in utero* VPA-induced ASD pathogenesis. The database of spontaneous behavior and basal LFP oscillation of VPA-exposed mice would be beneficial for further validation of the model. To investigate the spontaneous neural network activity, the LFPs were recorded from animals in individual's home cage as a highly familiar environment.

METHODS

Valproic acid (VPA) induced ASD in animals

This study was carried out in accordance with guidelines of the European Science Foundation (Use of Animals in Research 2001) and International Committee on Laboratory Animal Science, ICLAS (2004). The experimental protocols for care and use of experimental animals described in the present study were approved and guided by the Animals Ethical Committee of Prince of Songkla University (MOE 0521.11/287). All efforts were made to minimize animal suffering and to reduce the number of animals used.

The offspring with autism-like characteristics were produced by using a method described in the previous study (Cheaha et al. 2015). Briefly, the pregnant Swiss albino ICR mice received a single subcutaneous injection of 600 mg/kg sodium valproic acid (NaVPA) on embryogenesis day 13 (E13), while control dams received saline. Approximately 2–3 male pups per each litter were randomly selected from a total 8 litters (control or CTR: n=9, VPA: n=7). After birth, the pups

underwent a battery of behavioral tests as described previously (in supplement of Cheaha et al. 2015). During neonatal period (postnatal day 5–10), developmental milestones were examined including physical development and the neurodevelopmental reflexes. Therefore, neonatal ultrasonic vocalization (USV), spontaneous self-grooming behavior test and sociability test were also performed to validate the core behavioral phenotypes of ASD.

Surgery for intracranial electrode implantation

Method of intracranial electrode implantation was also previously described (Cheaha et al. 2015). Briefly, the silver wire electrodes (A–M system, Sequim, WA, USA) with bare diameter of 0.008" (Coated-0.011") were stereotaxically positioned (Fig. 3B) to the dorsal hippocampal CA1 [AP=−2.5 mm; ML=1.5 mm (left), DV=1.5 mm], the olfactory bulb [AP=+4.5 mm; ML=1 mm (left); DV=1.5 mm] and the medial prefrontal cortex [AP=+2.5 mm; ML=0.5 mm (left); DV=1.5 mm] according to the mouse brain atlas (Paxinos and Franklin 1998). The reference and ground electrodes were placed at midline above the cerebellum. Additional holes were drilled for stainless steel anchor screws. Dental acrylic was then used to secure and fix all electrodes on the skull. After surgery, animals were placed in a clean cage with a heating pad and monitored until ambulatory behavior was observed. The antibiotic ampicillin (General Drug House Co. Ltd., Thailand) was applied intramuscularly (100 mg/kg) once a day for 3 days to prevent infection.

The experimental setup and local field potential (LFP) recording

Animals were allowed to recover for at least 2 weeks and individually housed in a single standard home

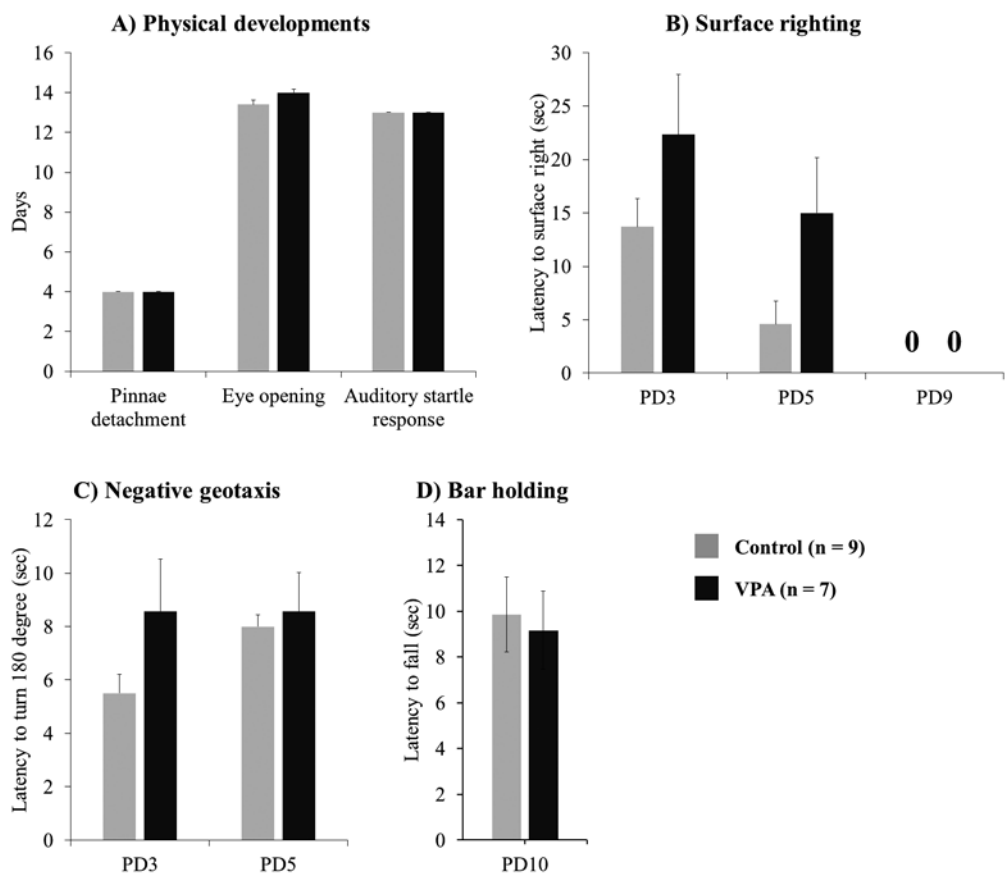

Fig. 1. Effects of *in utero* VPA exposure on general developmental milestones tests. From postnatal day (PD) 3–10, both control and prenatal VPA-exposed mice underwent a battery testing of developmental milestone including physical developments (A) surface righting (B), negative geotaxis (C) and bar holding (D).

cage (26×33×15 cm). LFPs and locomotor speed were recorded from animals in their home cage (Fig. 3A). For LFP recording, LFP signals were amplified with a low-pass 1 kHz, high-pass 0.1 by a PowerLab 16/35 system (AD Instruments, Australia) with 16-bit A/D. The data were then digitized at 2k Hz, stored and analyzed in a PC through the LabChart 7.3.7 Pro software (AD Instruments, Australia). Before LFP recording, animals were habituated for 2 hours per day in experimental room and connected to a dummy cable in their cage for 3 days before the experiment started. On the testing day, LFPs and locomotor activity of individual mice were recorded for 15 minutes. During the last 10 minutes, the animals exhibited more immobile and drowsy states. Therefore, the first 5-minute period of recording was selected for data analysis. This was in a purpose to have animals acclimatized to the recoding environment.

Locomotor speed (cm/sec) was recorded by using a video camera mounted on the top of the recording chamber. For the analysis, the images of moving animal were continuously transferred to a PC computer for data processing. The custom made computer software (visual C^{++}) developed in our lab was used to analyze animal movement (Cheaha et al. 2014).

Local field potential (LFP) data analysis

Raw signals were overviewed by using visual inspection and only noise-free signals were used for the analysis and processed through 1–100 Hz band passed digital filter. All LFP signal epochs were iden-

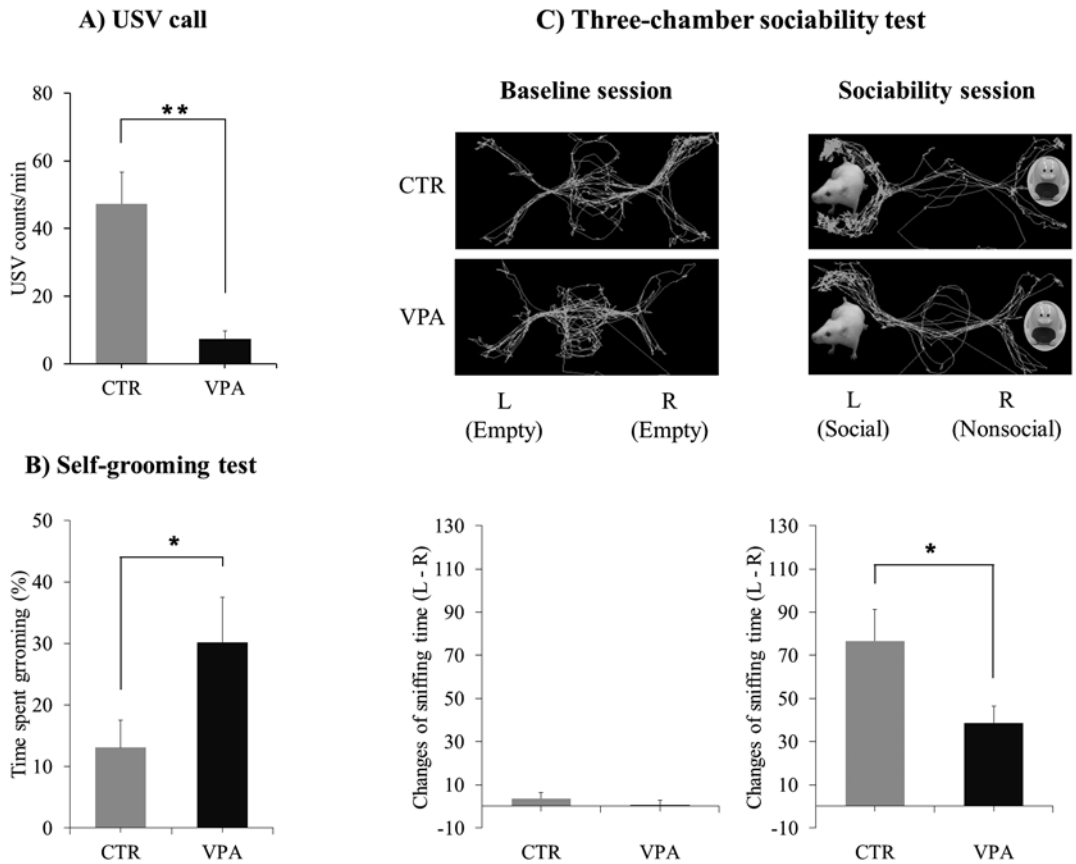

Fig. 2. The three core behavioral phenotypes were evaluated which include ultrasonic vocalization (USV) calls (A), time spent in spontaneous self-grooming (B) and three-chamber sociability test (C). During sociability test, animal's movement was tracked. Time spent sniffing in both sides during baseline session and sociability session was analyzed and expressed as changes of sniffing time by subtracting the left side (L) value with the right side (R) value. During baseline session, both left and right sides of the chamber were empty. A stranger mouse was put on the left side and object on the right side during sociability session. All data were calculated from 5-minute period recording and expressed as mean ±S.E.M. * indicates significant difference using unpaired Student t-test. * $P<0.05$, ** $P<0.01$.

tified in corresponding to behavioral states and locomotor speed which include the active exploratory state (speed>2 cm/sec) and awake-immobile state (speed=0 cm/sec).

Power spectral analysis

For spectral power analysis, LFP epochs>10-sec duration obtained during each behavioral states were selected to generate power spectral density (PSD) by LabChart software (PowerLab Software, AD Instruments, Castle Hill, Australia) using Hanning window cosine with 50% window overlap, and frequency resolution of 0.976 Hz. Then, the PSD in each frequency bin was expressed as percentage of total power (1–100 Hz). The average spectral powers were constructed in discrete frequency bands of each group and expressed in frequency domain based on correlations among frequency ranges and functional role of each brain areas.

Since several lines of evidence have supported hippocampal theta corresponding to exploratory behaviors (Whishaw and Vanderwolf, 1973), the hippocampal theta (4–12 Hz) oscillations were specifically analyzed in terms of theta peak power, theta peak frequency and mean theta frequency. Therefore, regres-

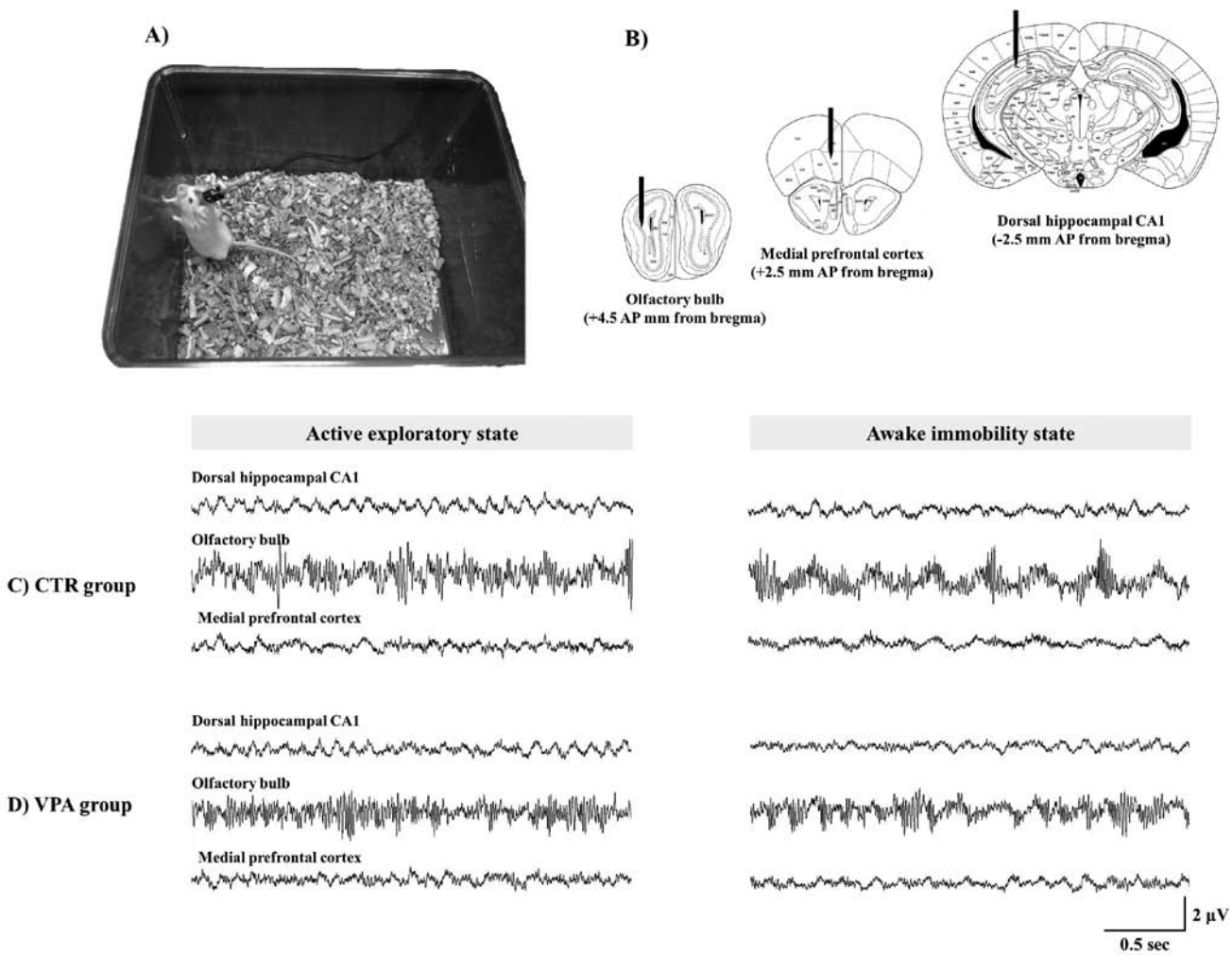

Fig. 3. Processes of LFP recording and analysis of *in utero* saline- (CTR) and VPA-treated mice during spontaneous activity in a highly familiar environment. (A) Individual animals were allowed to explore in the home cage. (B) Coronal mouse brain sections of the dorsal hippocampal CA1 (HP), the olfactory bulb (OB) and the medial prefrontal cortex (mPFC) show schematic drawings of silver wired electrode tip placements for LFP recording. Representative raw tracings of HP, OB and mPFC LFP during active exploratory and awake immobility states in CTR (C) and VPA (D) groups are shown.

sion analyzes were also performed between locomotor speed and hippocampal theta parameters during active exploratory state.

Coherence spectrogram analysis

The coherence spectrum is a measure for the interdependence of two signals in the frequency domain. The magnitude square coherences between two paired brain areas (hippocampus-olfactory bulb or hippocampus-medial prefrontal cortex) during active exploration and awake immobility were calculated by using Brainstorm3 software (Tadel et al. 2011) and expressed as coherence spectrogram. Coherence value ranges from zero to one. A value equals zero when the two signals are completely independent at the considered frequency. A value is one when the signals at specific frequency range are identical and have a constant phase relationship. The coherence values were averaged for selected frequency bands and compared between control and VPA groups.

Statistical analysis

All data were averaged and expressed as mean ±Standard Error of Mean (S.E.M.). Differences between the control (CTR) and VPA mice were analyzed by using two-way analysis of variance (ANOVA) with a treatment factors (CTR *vs.* VPA) and behavioral state factor (active exploratory vs awake immobility) followed by multiple comparisons with Tukey's *post hoc* test to indicate specific points of significance. In addition, linear regression analyses between hippocampal LFP powers and averaged locomotor speed were also analyzed. Levels of significance were set at $P<0.05$.

RESULTS

General developmental profiles and behaviors relevant to three core symptoms of ASD

During neonatal period (PD3–PD10), physical developments and neurodevelopmental reflexes were

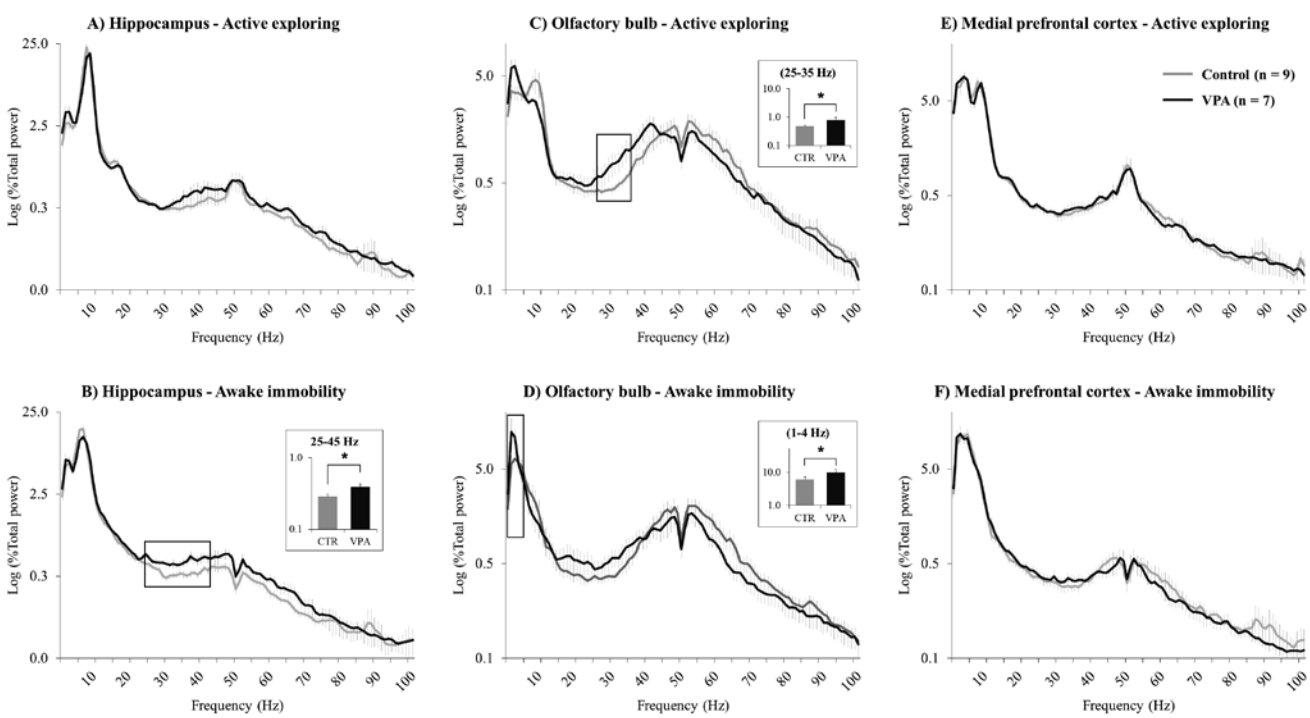

Fig. 4. Frequency analysis of hippocampal (A and B), olfactory bulb (C and D) and medial prefrontal cortex (E and F) LFP oscillations. Power spectral activity (percentage of total power) during spontaneous activity in a highly familiar environment of *in utero* saline- (CTR) and VPA-treated groups were expressed in frequency domain. The data during active exploration and awake immobility were separately analyzed. The influences of treatment and behavioral state factors were determined by using two-way ANOVA followed by Tukey's *post hoc* test. The insets indicate specific frequency ranges with significant difference between groups. Asterisks indicate significant difference (* $P<0.05$).

particularly analyzed. For physical developments, similar results of first day of pinnae detachment, eye opening and auditory startle response were found for both groups (Fig. 1A). There was no significant difference for these physical parameters. Moreover, surface righting reflex (Fig. 1B), negative geotaxis reflex (Fig. 1C) and bar holding (Fig. 1D) were analyzed for neurodevelopmental assessments. For surface righting reflex, ANOVA with repeated measures revealed a significant difference between groups for overall values ($F_{1,16}$=7.777, P<0.05). The data suggest a tendency of difference especially during PD3 and PD5. However, multiple comparisons with Tukey's *post hoc* test did not find any significant difference in each specific time point. Obviously, at PD9, animals from both groups exhibited the surface righting reflex without latent period. In addition, no significant difference was detected for both negative geotaxis reflex and bar holding tests.

To determine whether the VPA-exposed mice display autism-like characters, the three core behavioral characters of autism were analyzed (Fig. 2). First, the isolation-induced distress ultrasonic vocalization (USV) was recorded at PD12 to examine vocal communication activity. VPA-exposed mice exhibited significant reduction of the vocalization rate (t_{16}=3.901, P<0.01) (Fig. 2A). Secondly, at PD30, spontaneous self-grooming was tested to evaluate repetitive and compulsive behaviors. The VPA exposed group displayed a significant increase in time spent grooming behavior (t_{16}=−2.187, P<0.05) (Fig. 2B). Thirdly, at 4-month old, sociability was evaluated from three-chamber sociability test (Fig. 2C). Specific time spent sniffing a stranger mouse and the object was recorded. Both groups had similar baseline preference for left and right sides as seen during baseline session. However, on the sociability session, when a stranger mouse and an object were put into opposite chambers, VPA-exposed mice clearly had a significant decrease in time spent sniffing a stranger mouse in comparison to that of control mice (t_{16}=2.273, P<0.05).

Spontaneous basal local field potential (LFP) network oscillation in familiar environment

Local field potential (LFP) signals were recorded from animals during spontaneous activity in a highly familiar environment (Fig. 3A). Electrodes were placed into brain areas indicated (Fig. 3B). Representative raw LFP tracings of control and VPA animals were real-time monitored (Figs 3C and 3D, respectively). General appearances of LFPs revealed specific brain wave characters of active exploratory and awake immobility states. However, the differences between groups were not distinguished by visual inspection in any of these 3 brain areas (the hippocampus, the olfactory bulb and medial prefrontal cortex).

Power spectrum analysis of local field potentials (LFPs)

Frequency analysis of hippocampal LFP revealed specific character of power spectrums during active exploratory and awake-immobility states (Figs 4A and 4B, respectively). Theta (4–12 Hz) and gamma (30–100 Hz) oscillations were prominent especially during active exploration in both control and VPA groups. Two-way ANOVA revealed significant effects of treatment factors in theta (4–12 Hz) ($F_{1,31}$=5.479, P<0.05) and low gamma (25–45 Hz) ($F_{1,31}$=6.630,

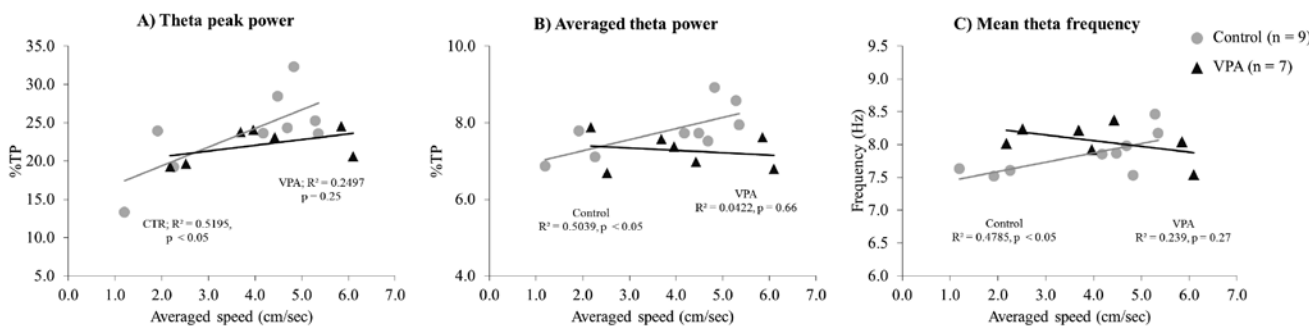

Fig. 5. Regression analyses between hippocampal theta oscillation and averaged speed during active exploration in a familiar environment. Theta activity was tested in terms of (A) maximal theta power, (B) average theta power and (C) averaged theta power.

P<0.05) frequency ranges. The effect of behavioral states showed significant effect on delta (1–4 Hz) ($F_{1,31}$=25.794, P<0.001) and theta ($F_{1,31}$=11.547, P<0.01) spectral power. However, interaction between both factors was not significant. Multiple comparisons using Tukey method indicated significant increase in low gamma power of VPA group during awake immobility state.

The olfactory bulb LFPs displayed different power spectrum patterns from that of hippocampal LFPs (Figs 4C and 4D). Two-way ANOVA revealed significant effects of treatment factors on delta (1–4 Hz) ($F_{1,31}$=5.374, P<0.05) and beta (25–35 Hz) ($F_{1,31}$=7.071, P<0.05) frequency ranges. Behavioral state had significant effect only on delta spectral power ($F_{1,31}$=10.545, P<0.01). Multiple comparison confirmed significant differences found in beta range during active exploration and delta range during awake immobility.

Power spectrums of medial prefrontal cortex LFP were analyzed (Figs 4E and 4F). Relatively similar patterns between groups were seen. Factors of treatment had no significant effect on spectral power in this brain area.

Correlations between hippocampal theta local field potential (LFP) oscillations and locomotor speed during active exploration

In general, hippocampal oscillation can be related either with cognitive or sensorimotor functions. Regression analyzes were performed to evaluate the associations between hippocampal theta oscillations and locomotor speed (a sensorimotor component) during active exploration. In control group, significant correlations were observed between averaged speed and theta peak power (R^2=0.52, P<0.05), averaged

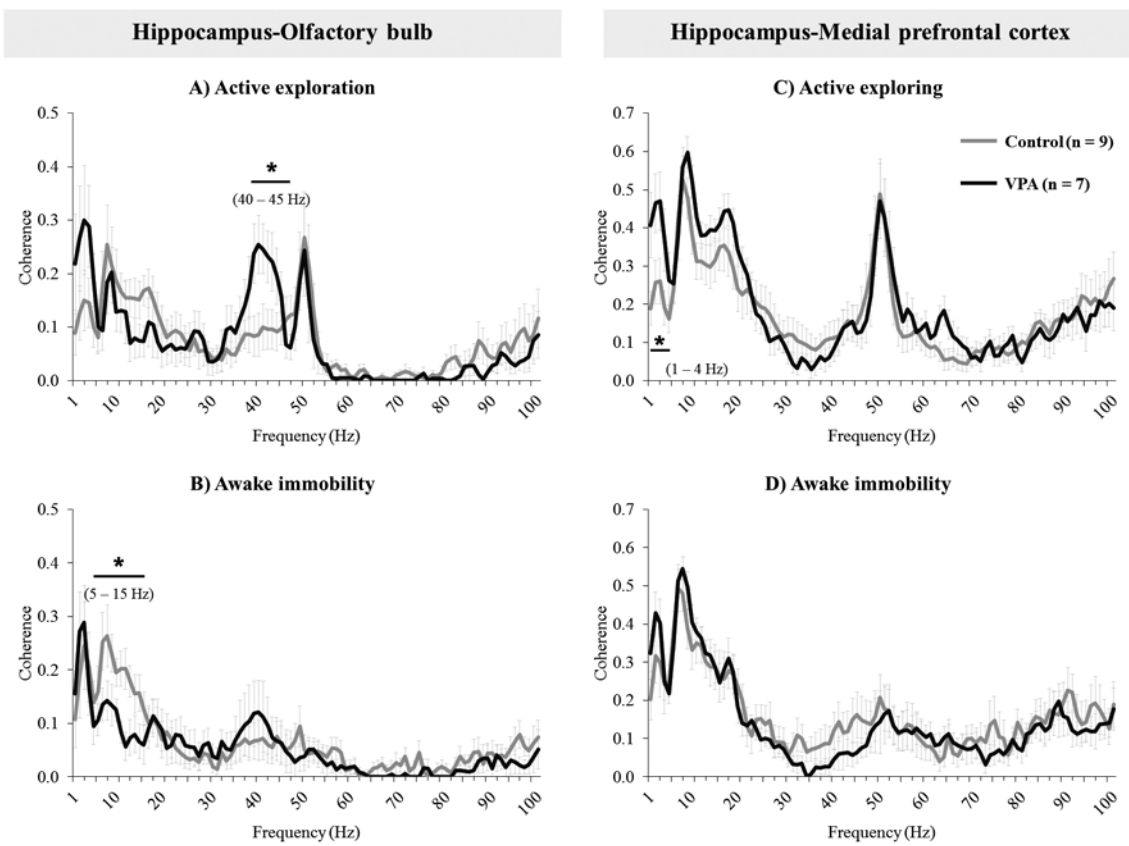

Fig. 6. Coherence spectrograms between LFP signals from the hippocampus and related brain areas (olfactory bulb and medial prefrontal cortex). Averaged values were plotted for data from two pairs of brain areas during active exploration and awake immobility (A–D). The influences of treatment and behavioral state factors were determined by using two-way ANOVA followed by Tukey's *post hoc* test. Asterisks indicate significant difference between CTR and VPA groups (* P<0.05).

theta power (R^2=0.50, P<0.05) and mean theta frequency (R^2=0.48, P<0.05) (Figs 5A–5C respectively). However, the averaged speed in VPA group failed to predict hippocampal theta LFP oscillations for these parameters.

Coherence analysis

The oscillations of two sources with the same frequency were evaluated to confirm the interplay between separate areas. Values of coherence between two brain areas were analyzed for 1–100 Hz range. The results showed that coherence between the hippocampus and the olfactory bulb of VPA group was significantly increased within gamma frequency range (40–45 Hz) during active exploration ($F_{1,31}$=3.996, P<0.05) (Fig. 6A) and decreased within theta frequency range (5–15 Hz) during awake immobility ($F_{1,31}$=5.265, P<0.05) (Fig. 6B). Significant increase in coherence between the hippocampus and the medial prefrontal area of VPA group was also seen in delta frequency range (1–4 Hz) during active exploration ($F_{1,31}$=6.105, P<0.05) (Fig. 6C). No significant difference in coherence between groups for these two areas was seen during awake immobility (Fig. 6D).

DISCUSSION

The present data support the validity of valproic acid (VPA) mouse model of autism spectrum disorders (ASDs). Overall behavioral data confirmed specific characteristics of ASD induced by *in utero* VPA exposure including a reduction of ultrasonic vocalization, poor sociability and increased self-grooming behavior. These were in agreement with previous works (Gandal et al. 2010, Favre et al. 2013). Taken together, the mouse offspring in this study were suitable for investigation of neuronal network function. This might also indicate a possible translatability of the VPA mouse model for clinical research of autism.

In this study, signal processing tool was employed to investigate neural network signaling in order to understand information processing in autism. Most of the findings were obtained from animals being tested with challenges (Cheaha et al. 2015). These data seemed to suggest abnormal signal processing in animals while performing a novel test. However, it is necessary to examine whether autism behavior is due to disruption of the learning-associated neural circuits that would also exert differential signaling during basal activity. Until recently, basal signaling in learning related brain areas of ASD animal model has not been explored. The LFPs from all 3 brain areas which included the hippocampus (HP), the olfactory bulb (OB) and the medial prefrontal cortex (mPFC) were recorded in animals in individual's home cage to investigate spontaneous neural network activity. With this condition, it would be able to characterize neural signaling as a surrogate biomarker linked to learning impairment in VPA mouse model.

From raw LFP signals, VPA animals displayed relatively normal LFP oscillation patterns in all 3 brain areas during both active exploratory and awake immobile states. Hippocampal theta wave (4–12 Hz) was predominantly observed in both control and VPA animals during active exploratory behavior. Moreover, VPA group also exhibited gamma bursts in the olfactory bulb similarly to that seen in control group. No pathological oscillation including spike or sharp-wave epileptiform was found in VPA mice. These findings suggest that, visual inspection of raw LFP signals seemed unlikely to distinguish neural signaling of VPA from that of control animals. This suggests that modern algorithms are needed to investigate subtle modifications of signaling process in the brain of VPA mouse model.

Frequency analysis of all LFP signals during both active exploring and awake immobility also revealed modest differences in power spectrums in VPA mice. The increased hippocampal low gamma power (25–45 Hz) during awake immobile was observed in VPA mice. This indicated basal oscillation of hippocampal network affected by *in utero* VPA exposure. Previously, the hippocampal network activity of VPA mouse model of ASD was examined in response to a novel environment. The analysis revealed the increases in slow wave (1–4 Hz) and high gamma (80–100 Hz) oscillations and decrease in theta (4–12 Hz) activity in the hippocampus (Cheaha et al. 2015).

In general, gamma oscillations have been associated with sensory gating impairment (Orekhova et al. 2008), cortical hyperexcitability (Cheaha et al. 2014) or an excitatory/inhibitory imbalance (Gogolla et al. 2009). However, the underlying mechanism of hippocampal signal processing in VPA mouse model remained uninvestigated. Mostly, consequences of prenatal VPA exposure on the hippocampus have been studied in cellular and molecular levels. Previously,

histological studies demonstrated the effects of prenatal VPA exposure on the hippocampus including altered glutamate metabolism (Bristot Silvestrin et al. 2013), decreased neuroligin 3 mRNA expression (Kolozsi et al. 2009) and reduced CA1 layer thickness (Sosa-Díaz et al. 2014). Disruptions of hippocampal network plasticity might have impacts on the intrinsic oscillatory activity under basal conditions.

Previous studies have shown that hippocampal theta power and frequency were strongly modulated by running speed (Shin et al. 2001). These indicate the integration of locomotor-related spatial information of hippocampal processing. In this study, locomotor speed related hippocampal theta activity seemed to be altered while VPA animals exploring in home cage. However, in a novel environment, a positive correlation between theta oscillation and maximal locomotor speed was evidenced (Cheaha et al. 2015). These data suggest a wide range of functional theta oscillations in the hippocampus of this VPA mouse model. The correlation with locomotor activity seemed to be absent in resting state and restored by challenging with a novel situation that would enhance exploration. Moreover, locomotor speed related theta activity can be detected even though percent total power of theta frequency was unchanged.

Changes of spectral power activity were observed in the olfactory bulb of VPA animals but not the medial prefrontal cortex. In olfactory bulb LFP, VPA animals also displayed distinct oscillation patterns during both active exploration and awake immobility. Previously, *in utero* VPA-exposed animals also displayed differential olfactory bulb oscillations in response to novel environment (Cheaha et al. 2015). This might reflect an impairment of olfactory function induced by *in utero* VPA exposure reported in previous studies (Murray et al. 2011, Favre et al. 2013, Kolozsi et al. 2009).

Analysis of magnitude square coherence was expected to demonstrate the indices of functional connectivities between difference brain areas. In this study, *in utero* VPA exposure led to distinct interplays between brain areas within specific frequency ranges of LFP. Coherence analysis revealed an increased coherence between the hippocampus and the olfactory bulb within gamma range (40–45 Hz) and decreased within 5–15 Hz frequency range in VPA animals during active exploration and awake immobility, respectively. Previously, basal communication within olfacto-hippocampal network system was also observed in some rhythmically synchronized activities. Slow oscillation (2–4 Hz) of the hippocampus was entrained by nasal respiration in urethane-anesthetized mice (Yanovsky et al. 2014). In addition, odor stimulation was found to strongly enhance beta activity (15–35 Hz) in the hippocampus (Martin et al. 2007). However, the present findings also revealed a weak interplay between the hippocampus and the olfactory bulb (theta frequency, 6–12 Hz). It means that the communication between them either in feedforward or feedback directions is low.

VPA animals also displayed an increased coherence between the hippocampus and the prefrontal cortex within delta frequency range (1–4 Hz) during active exploration. Hippocampal–prefrontal synchrony deficits have been reported in various animal models including schizophrenia mouse model that power spectral analysis did not show significant change (Sigurdsson et al. 2010). Abnormal coherence between the medial prefrontal cortex and the hippocampus in correlation with sensory gating was seen in animal model of schizophrenia (Dickerson et al. 2010, 2012). In this model, coherence in the delta range (1–4 Hz) of hippocampal-prefrontal synchrony was reported especially during spatial working memory test (Sigurdsson et al. 2010).

Processing of information in the central nervous system appears to be carried out through various brain rhythms as fundamental mechanisms. Neural oscillations have been proposed to be important for information transfer between separate brain areas (Uhlhaas et al. 2009). LFP synchronizations between distant neuronal groups would represent frameworks of brain circuit necessary for cognitive functions (Buzsaki 2010). In this study, signal processing tool was employed to investigate neural network signaling especially in the neural networks associated with learning process. In terms of brain regions involved in neuropathology of autism, the mPFC and the olfactory bulb are among potential candidates in addition to the hippocampus.

Cellular and molecular alteration of learning-related brain circuit including the hippocampus, the olfactory bulb (Kolozsi et al. 2009) and the medial prefrontal cortex (Hara et al. 2015, Kim et al. 2013) of VPA animals have been reported. However, a few studies have examined functional network activity of these brain areas. Previously, neural circuit hyperactivity was observed in various brain areas of *in utero* VPA ani-

mals including the somatosensory cortex, the prefrontal cortex (Silva et al. 2009) and the lateral amygdala (Markram et al. 2007). In this study, disrupted LFP patterns in the hippocampal CA1, the olfactory bulb and the medial prefrontal cortex were also demonstrated in mice prenatally exposed to VPA. Changes of LFP power might be associated with local circuit dysfunction. Previously, electrophysiological abnormalities have been proposed to underlie network hyperactivity within hyperconnected microcircuits (Rinaldi et al. 2007, 2008). Altogether, the present spectral power analysis highlighted the disrupted signaling in the hippocampus and the olfactory bulb of VPA-exposed animals.

In addition to neural signaling in individual brain regions, the interplays between brain areas have been studied to understand functional connections as frameworks of neuronal network. The network formed by the hippocampus and the olfactory bulb appeared to represent an ideal model of social learning in mouse models as rodents recognize each other by using olfactory sense mainly (Lin et al. 2005). Additionally, the medial prefrontal area in rodents also plays a role in modulating social interaction (Uylings et al. 2003). The present study demonstrated distinct interplays between the hippocampus and learning-related brain areas which included the olfactory bulb and the medial prefrontal cortex. In a rat model of autism, differential structural connectivity between the mPFC and the hippocampus was demonstrated (Codagnone et al. 2015). However, changes in LFP coherence between these two areas in VPA mouse model were not examined. Deficits in synaptic maturation and excitatory/inhibitory imbalance were hypothesized to be the underlying mechanisms of disrupted functional connectivity in ASD (Rubenstein and Merzenich 2003, Baudouin et al. 2012). Therefore, these mechanisms might be associated with abnormal coherences found in VPA mice shown in this study.

CONCLUSION

The present study supported the validity of animal model of autism induced by *in utero* VPA exposure with physical and neurodevelopmental data. Particularly, three core characters of autism were induced by *in utero* VPA. This study highlighted distinct neural signaling in VPA mouse model of autism. Spectral power analysis was performed to determine signaling disruptions in individual brain areas whereas coherence analysis was for the investigation of functional connectivity between two separate areas. These findings confirmed that disruptions of individual or both brain regions connected were found to affect the LFP coherences in VPA mouse model of ASD. The LFP oscillation patterns clearly characterized specific endophenotypes of VPA mouse model and provided basal neural signaling in learning-related brain areas of autism-like animals.

ACKNOWLEDGEMENTS

This work was financially supported by grants from graduated school, The Department of Physiology, the Faculty of Science, Prince of Songkla University, Hatyai, Songkhla, 90112, Thailand and the research professional development project under the science achievement scholarship of Thailand (SAST).

REFERENCES

American Psychiatric Association (2013) Diagnostic and statistical manual of mental disorders: DSM-5. American Psychiatric Association, Washington D.C., USA.

Baudouin SJ, Gaudias J, Gerharz S, Hatstatt L, Zhou K, Punnakkal P, Tanaka KF, Spooren W, Hen R, De Zeeuw CI, Vogt K, Scheiffele P (2012) Shared synaptic pathophysiology in syndromic and nonsyndromic rodent models of autism. Science 338: 128–132.

Bristot Silvestrin R, Bambini-Junior V, Galland F, Daniele Bobermim L, Santos A, Torres Abib R, Zanotto C, Batassini C, Brolese G, Gonçalves CA, Riesgo R, Gottfried C (2013) Animal model of autism induced by prenatal exposure to valproate: Altered glutamate metabolism in the hippocampus. Brain Res 1495: 52–60.

Buzsaki G (2010) Neural syntax: cell assemblies, synapsembles, and readers. Neuron 68: 362–385.

Chaste P, Leboyer M (2012) Autism risk factors: genes, environment, and gene-environment interactions. Dialogues Clin Neurosci 14: 281–292.

Cheaha D, Bumrungsri S, Chatpun S, Kumarnsit E (2015) Characterization of *in utero* valproic acid mouse model of autism by local field potential in the hippocampus and the olfactory bulb. Neurosci Res 98: 28–34.

Cheaha D, Sawangjaroen K, Kumarnsit E (2014) Characterization of fluoxetine effects on ethanol withdrawal-induced cortical hyperexcitability by EEG spectral power in rats. Neuropharmacology 77: 49–56.

Codagnone MG, Podesta MF, Uccelli NA, Reines A (2015) Differential Local Connectivity and Neuroinflammation Profiles in the Medial Prefrontal Cortex and Hippocampus in the Valproic Acid Rat Model of Autism. Dev Neurosci 37: 215–231.

Dickerson DD, Restieaux AM, Bilkey DK (2012) Clozapine administration ameliorates disrupted long-range synchrony in a neurodevelopmental animal model of schizophrenia. Schizophr Res 135: 112–115.

Dickerson DD, Wolff AR, Bilkey DK (2010) Abnormal long-range neural synchrony in a maternal immune activation animal model of schizophrenia. J Neurosci 30: 12424–12431.

European Science Foundation (2001) Use of Animals in Research. http://www.esf.org/fileadmin/Public_do.

Favre MR, Barkat TR, LaMendola D, Khazen G, Markram H, Markram K (2013) General developmental health in the VPA-rat model of autism. Front Behav Neurosci 7: 88.

Gandal MJ, Edgar JC, Ehrlichman RS, Mehta M, Roberts TP, Siegel SJ (2010) Validating gamma oscillations and delayed auditory responses as translational biomarkers of autism. Biol Psychiatry 68: 1100–1106.

Gogolla N, LeBlanc JJ, Quast KB, Südhof TC, Fagiolini M, Hensch TK (2009) Common circuit defect of excitatory-inhibitory balance in mouse models of autism. J Neurodev Disord 1: 172–181.

Hara Y, Takuma K, Takano E, Katashiba K, Taruta A, Higashino K, Hashimoto H, Ago Y, Matsuda T (2015) Reduced prefrontal dopaminergic activity in valproic acid-treated mouse autism model. Behav Brain Res 1: 39–47.

National Research Council Institute for Laboratory Animal Research (2004) The Development of Science-based Guidelines for Laboratory Animal Care: Proceedings of the November 2003 International Workshop. National Academies Press, Washington DC, USA.

Jamain S, Quach H, Betancur C, Rastam M, Colineaux C, Gillberg IC, Soderstrom H, Giros B, Leboyer M, Gillberg C, Bourgeron T (2003) Mutations of the X-linked genes encoding neuroligins NLGN3 and NLGN4 are associated with autism. Nat Genet 34: 27–29.

Kim KC, Kim P, Go HS, Choi CS, Park JH, Kim HJ, Jeon SJ, dela Pena IC, Han SH, Cheong JH, Ryu JH, Shin CY (2013) Male-specific alteration in excitatory post-synaptic development and social interaction in pre-natal valproic acid exposure model of autism spectrum disorder. J Neurochem 124: 832–843.

Kim KC, Kim P, Go HS, Choi CS, Yang SI, Cheong JH, Shin CY, Ko KH (2011) The critical period of valproate exposure to induce autistic symptoms in Sprague-Dawley rats. Toxicol Lett 201: 137–142.

Kolozsi E, Mackenzie RN, Roullet FI, Decatanzaro D, Foster JA (2009) Prenatal exposure to valproic acid leads to reduced expression of synaptic adhesion molecule neuroligin 3 in mice. Neuroscience 163: 1201–1210.

Lin DY, Zhang SZ, Block E, Katz LC (2005) Encoding social signals in the mouse main olfactory bulb. Nature 434: 470–477.

Markram K, Rinaldi T, Mendola DL, Sandi C, Markram H (2007) Abnormal Fear Conditioning and Amygdala Processing in an Animal Model of Autism. Neuropsychopharmacology 33: 901–912.

Martin C, Beshel J, Kay LM (2007) An Olfacto-hippocampal network is dynamically involved in odor-discrimination learning. J Neurophysiol 98: 2196–2205.

Meador KJ, Baker GA, Browning N, Clayton-Smith J, Combs-Cantrell DT, Cohen M, Kalayjian LA, Kanner A, Liporace JD, Pennell PB, Privitera M, Loring DW (2009) Cognitive function at 3 years of age after fetal exposure to antiepileptic drugs. N Engl J Med 360: 1597–1605.

Miyazaki K, Narita N, Narita M (2005) Maternal administration of thalidomide or valproic acid causes abnormal serotonergic neurons in the offspring: implication for pathogenesis of autism. Int J Dev Neurosci 23: 287–297.

Moldrich RX, Leanage G, She D, Dolan-Evans E, Nelson M, Reza N, Reutens DC (2013) Inhibition of histone deacetylase in utero causes sociability deficits in postnatal mice. Behav Brain Res 257: 253–264.

Murray EK, Varnum MM, Fernandez JL, de Vries GJ, Forger NG (2011) Effects of neonatal treatment with valproic acid on vasopressin immunoreactivity and olfactory behaviour in mice. J Neuroendocrinol 23: 906–914.

Narita M, Oyabu A, Imura Y, Kamada N, Yokoyama T, Tano K, Uchida A, Narita N (2010) Nonexploratory movement and behavioral alterations in a thalidomide or valproic acid-induced autism model rat. Neurosci Res 66: 2–6.

Ornoy A (2009) Valproic acid in pregnancy: How much are we endangering the embryo and fetus?. Reprod Toxicol 28: 1–10.

Orekhova EV, Stroganova TA, Prokofyev AO, Nygren G, Gillberg C, and Elam M (2008) Sensory gating in young children with autism: Relation to age, IQ, and EEG gamma oscillations. Neurosci Lett 434: 218–223.

Paxinos G, Franklin KBJ (1998) The mouse brain in stereotaxic coordinates. Academic Press, San Diego–California–London, USA–UK.

Phiel CJ, Zhang F, Huang EY, Guenther MG, Lazar MA, Klein PS (2001) Histone deacetylase is a direct target of

valproic acid, a potent anticonvulsant, mood stabilizer, and teratogen. J Biol Chem 276: 36734–36741.

Rice D, Barone S (2000) Critical periods of vulnerability for the developing nervous system: evidence from humans and animal models. Environ Health Perspect 3: 511–533.

Rinaldi T, Kulangara K, Antoniello K, Markram H (2007) Elevated NMDA receptor levels and enhanced postsynaptic long-term potentiation induced by prenatal exposure to valproic acid. Proc Natl Acad Sci U S A: 13501–13506.

Rinaldi T, Perrodin C, Markram H (2008) Hyper-Connectivity and Hyper-Plasticity in the Medial Prefrontal Cortex in the Valproic Acid Animal Model of Autism. Front Neural Circuits 2: 4.

Rubenstein JLR, Merzenich MM (2003) Model of autism: increased ratio of excitation/inhibition in key neural systems. Genes Brain Behav 2: 255–267.

Schneider T, Przewłocki R (2004) Behavioral alterations in rats prenatally exposed to valproic acid: animal model of autism. Neuropsychopharmacology 30: 80–89.

Shen C, Huo LR, Zhao XL, Wang PR, Zhong N (2015) Novel interactive partners of neuroligin 3: new aspects for pathogenesis of autism. J Mol Neurosci 56: 89–101.

Shin J, Talnov A, Matsumoto G, Brankack J (2001) Hippocampal theta rhythm and running speed: A reconsideration using within-single trial analysis. Neurocomputing 38: 1567–1574.

Sigurdsson T, Stark KL, Karayiorgou M, Gogos JA, Gordon JA (2010) Impaired hippocampal-prefrontal synchrony in a genetic mouse model of schizophrenia. Nature 464(7289): 763–767.

Silva GT, Le Bé JV, Riachi I, Rinaldi T, Markram K, Markram H (2009) Enhanced long term microcircuit plasticity in the valproic acid animal model of autism. Front Synaptic Neurosci 1: 1.

Sosa-Díaz N, Bringas ME, Atzori M, Flores G (2014) Prefrontal cortex, hippocampus, and basolateral amygdala plasticity in a rat model of autism spectrum. Synapse 68: 468–473.

Strömland K, Nordin V, Miller M, Akerström B, Gillberg C (1994) Autism in thalidomide embryopathy: a population study. Dev Med Child Neurol 36: 351–356.

Tadel F, Baillet S, Mosher JC, Pantazis D, Leahy RM (2011) Brainstorm: A user-friendly application for MEG/EEG analysis. Comput Intell Neurosci 2011: 879716.

Uhlhaas PJ, Roux F, Singer W, Haenschel C, Sireteanu R, Rodriguez E (2009) The development of neural synchrony reflects late maturation and restructuring of functional networks in humans. Proc Natl Acad Sci U S A 106: 9866–9871.

Uylings HB, Groenewegen HJ, Kolb B (2003) Do rats have a prefrontal cortex?. Behav Brain Res 146: 3–17.

Volk HE, Kerin T, Lurmann F, Hertz-Picciotto I, McConnell R, Campbell DB (2014) Autism spectrum disorder: interaction of air pollution with the MET receptor tyrosine kinase gene. Epidemiology 25: 44–47.

Vorhees CV, Rauch SL, Hitzemann RJ (1991) Prenatal valproic acid exposure decreases neuronal membrane order in rat offspring hippocampus and cortex. Neurotoxicol Teratol 13(4): 471–474.

Whishaw IQ, Vanderwolf CH (1973) Hippocampal EEG and behavior: Change in amplitude and frequency of RSA (Theta rhythm) associated with spontaneous and learned movement patterns in rats and cats. Behav Biol 8: 461–484.

Williams G, King J, Cunningham M, Stephan M, Kerr B, Hersh JH (2001) Fetal valproate syndrome and autism: additional evidence of an association. Dev Med Child Neurol 43: 202–206.

Willsey AJ, Sanders SJ, Li M, Dong S, Tebbenkamp AT, Muhle RA, Reilly SK, Lin L, Fertuzinhos S, Miller JA, Murtha MT, Bichsel C, Niu W, Cotney J, Ercan-Sencicek AG, Gockley J, Gupta A, Han W, He X, Hoffman E, Klei L, Lei J, Liu W, Liu L, Lu C, Xu X, Zhu Y, Mane SM, Lein ES, Wei L, Noonan JP, Roeder K, Devlin B, Sestan N, State M (2013) Coexpression networks implicate human midfetal deep cortical projection neurons in the pathogenesis of autism. Cell 155: 997–1007.

Yanovsky Y, Ciatipis M, Draguhn A, Tort AB, Brankačk J (2014) Slow oscillations in the mouse hippocampus entrained by nasal respiration. J Neurosci 34(17): 5949–5964.